

Seit 1993 verfolgt das südafrikanische Energieversorgungsunternehmen Eskom die Entwicklung eines Modularen Kugelhaufenreaktors (PBMR) mit internationalen Kooperationspartnern.

Der PBMR ist das am weitesten entwickelte Projekt im Rahmen der Generation IV Hochtemperaturreaktorentwicklung. Erstes Ziel ist die Errichtung einer Demonstrationsanlage mit 110 MWe elektrischer Leistung am Standort Koeberg nahe Kapstadt. Dort werden derzeit die zwei einzigen Kernkraftwerke des Landes betrieben.

Das Grundkonzept sieht vor, Einheiten von jeweils ca. 165 MW Leistung zu errichten, die zu Gesamtsystemen von 2, 4 oder 8 Blöcken zusammengefasst werden können.

Das technische Grundkonzept des PBMR basiert auf einem Druckbehälter aus Stahl mit Graphit-Liner und kugelförmigen Brennelementen, die den Kernbrennstoff als Coated Particles enthalten. Als Kühlmittel wird Helium eingesetzt, das in einem dreistufigen Brayton-Cycle zum Betrieb des Generators in einem Helium-Direkt-Kreislauf genutzt wird.

Die Anlagenkonzeption gewährleistet höchste Sicherheit, da kein Risiko einer Freisetzung größerer Aktivitätsmengen gegeben ist.

Ein wichtiger Schritt in der PBMR-Entwicklung sind Inbetriebnahme und erste erfolgreiche Versuche einer Testeinrichtung für den vorgesehenen Kühlkreislauf der Helium-Direkt-Turbine an der Faculty of Engineering der Potchefstroom University (Südafrika) mit begleitenden thermodynamischen Analysen.

Darüber hinaus wird auch mit den aktuellen Ergebnissen das weitere Projektvorgehen untersucht.

Anschriften der Verfasser:

Prof. G.P. Greyvenstein and

Prof. P.G. Rousseau

Department of Mechanical Engineering
Potchefstroom University for Christian
Higher Education (PU for CHE), Private
Bag X6001, Potchefstroom 2520,
Republic of South Africa

Dr. Dave Nicholls

Chief Executive officer, PBMR Pebble
Bed Modular Reactor (Pty) Ltd.
3rd Floor Lake Buena Vista Building,
1267 Gordon Hood Avenue, Centurion,
Republic of South Africa

Design and Successful Testing of a Physical Model of the Pebble Bed Modular Reactor

G.P. Greyvenstein and P.G. Rousseau, Potchefstroom
Dave Nicholls, Centurion, Republic of South Africa

Introduction

The South African utility *Eskom* has been investigating the PBMR technology since 1993 for potential application as a power source in South Africa, as well as a viable South African export product. *Eskom's* partners are the *South African Industrial Development Corporation* and *BNFL*.

The South African PBMR is the most advanced within the Generation IV HTGR (High Temperature Gas Cooled) Reactors to be designed for commercial purposes. The intention is to build a 110 MWe class demonstration PBMR at Koeberg near Cape Town, where Africa's only nuclear power plant is situated; and an associated fuel plant at Pelindaba near Pretoria, where fuel for Koeberg used to be manufactured.

The concept allows for additional modules to be added in accordance with demand and to be configured to the size required by the communities they serve. It can operate in isolation anywhere, provided that there is sufficient water for cooling. Dry cooling, although more expensive, is an option that would provide even more freedom of location.

The commercial reactors would be sized to produce about 165 MW each. To maximise the sharing of support systems, however, the PBMR has been configured into a variety of options, such as 2, 4 and 8-pack layouts. These are the most cost ef-

fective layouts and allow the plants to be brought on line as they are completed.

The PBMR reactor consists of a vertical steel pressure vessel lined with graphite bricks. It uses silicon carbide coated particles of enriched uranium oxide encased in graphite to form a fuel sphere or pebble, hence its name. The PBMR is based on closed cycle three-shaft recuperative Brayton cycle and it uses helium as the coolant and energy transfer medium.

PBMR fuel is based on a proven high-quality German fuel design consisting of Low Enriched Uranium Triple-coated Isotropic (LEU-TRISO) particles contained in a molded graphite sphere. A coated particle consists of a kernel of uranium dioxide surrounded by four coating layers.

The PBMR represents a significant advance in nuclear safety. In respect of "conventional" power reactors, the probability of a large release of radioactivity is minimal. In addition, the associated risk to near-by populations is several orders of magnitude less than non-nuclear risks accepted without question in daily life. In respect of the PBMR, there is no risk of a major release – short of total destruction of the plant by an outside agency. Because the PBMR system is, to a high degree, inherently safe, there is less need for the sophisticated and costly engineered safety systems that surround today's large power reactors. The PBMR therefore also promises significantly cheaper power than its predecessors.

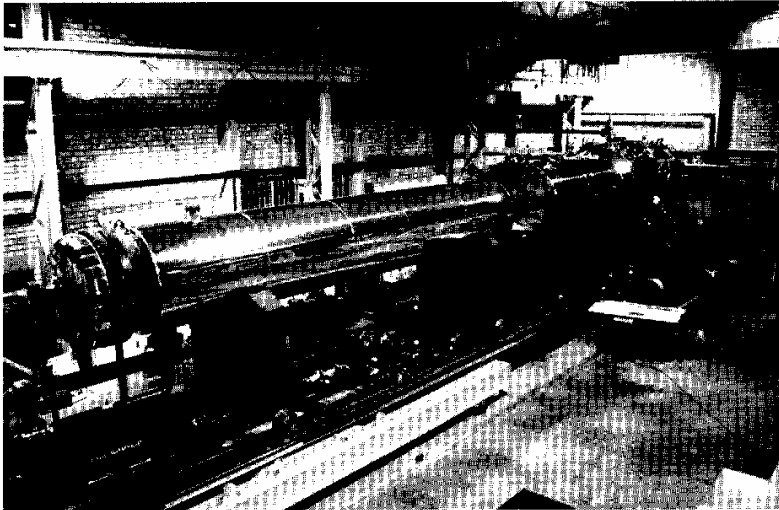


Fig 1. Test Rig of the PBMR power conversion system.

Project status

The environmental impact assessment (EIA) process was concluded in October 2002 and the final reports submitted to the South Africa Department of Environmental Affairs and Tourism. In addition to approval by the investors and a positive Record of Decision on the EIA, proceeding to the next phase (building of a demonstration module and associated fuel plant) is subject to the issuing of a construction license by the South African National Nuclear Regulator and Government consent.

The PBMR investors are currently reviewing the business case and will in due course decide on the way forward.

Test rig of the power conversion system

An important milestone was recently reached with the successfully start-up of a test rig of the PBMR power conversion system. It is believed that the test rig, or micro turbine model, represents the first closed-cycle, multi-shaft gas turbine in the world.

The micro model (Figure 1) was designed and built by the Faculty of Engineering at Potchefstroom University near Johannesburg, with technical input from the PBMR project team.

The test rig is a replica of the functional layout of the PBMR power plant with the same control topology and degrees of freedom as the PBMR plant. It will fairly accurately predict the behaviour of the power plant and addresses one of the main technical risks of the project, namely the integrated controllability of a multi-shaft system. Furthermore, the

PBMR-developed thermal hydraulic design code Flownet accurately predicted various plant parameters, providing a major boost of confidence in the technical feasibility of the PBMR concept.

The main objectives of the micro model project were to prove that a three shaft recuperated Brayton cycle can be sustained and controlled, that it renders a stable operating configuration and to provide code verification. The four control philosophies of the PBMR identified for demonstration were start-up, full power operation, load following and load rejection.

Although it is relatively easy to predict the steady-state performance of a plant such as the PBMR, the prediction of the dynamic behaviour of the PBMR, which is required for the design of the control system, presents unique challenges. A great effort was therefore put into the development of a powerful new dynamic modelling tool, called Flownet.

One of the distinguishing features of the PBMR is the use of three separate shafts for the different compressor/turbine and turbine/generator pairs as opposed to one or two shafts used in other designs. This, however, complicates the design of the control system.

In order to test the control strategies of the PBMR and also to demonstrate the accuracy of Flownet, it was decided to develop a micro model of the power conversion cycle. The model uses an electrical heater to emulate the nuclear reactor. Since the objective of the micro model is not to address specific issues related to the use of helium as the working fluid or to test the performance of individual components such as compressors, turbines or heat exchangers, it was decided to use nitrogen instead of helium as the working fluid.

This makes it possible to use off-the-shelf, single stage centrifugal compressors and turbines instead of more expensive multi-stage centrifugal or axial flow machines. It should be stressed that the micro model is not a scale model of the prototype plant but a system that will have the same characteristics and degrees of freedom and therefore also the same control topology as the prototype plant.

Power conversion cycle and comparison with the micro model

A schematic layout of the PBMR power conversion cycle is shown in Figure 2. Starting at 1, helium at a relatively low pressure and temperature is compressed by a low-pressure compressor (LPC) to an intermediate pressure (2) after which it is cooled in an intercooler to state 3. A high-pressure compressor (HPC) then compresses the helium to state 4. From 5 to 6 the helium is preheated in the recuperator before entering the reactor, which heats the helium to state 8. After the reactor, the hot high-pressure helium is expanded in a high-pressure turbine (HPT) to state 9 after which it is further expanded in a low-pressure turbine (LPT) to state 11. The high-pressure turbine drives the high-pressure compressor while the low-pressure turbine drives the low-pressure compressor. After the low pressure turbine, the helium is further expanded in the power turbine to pressure 13. From 13 to 14 the still hot helium is cooled in the recuperator, after which it is further cooled in the pre-cooler to state 1. This completes the cycle. The heat rejected from 13 to 14 is equal to the heat transferred to the helium from 5 to 6.

The output of the plant can be controlled by changing the helium inventory of the system or by opening and closing of the bypass valve (BPV). Changing of the helium inventory is a relatively slow process and is used for load following, while the faster bypass control is used for load rejection.

Although the design of the micro model closely resembles that of the PBMR plant, the following differences should be noted:

- (i) The micro model uses nitrogen instead of helium as the working fluid. This does not detract from the objective of the model, namely to develop a system that will have the same overall characteristics as that of the prototype plant rather than to address specific issues related to the use of helium as the working fluid.
- (ii) The micro model uses cheap, off-the-shelf, single-stage, centrifugal compressors and turbines rather than axial

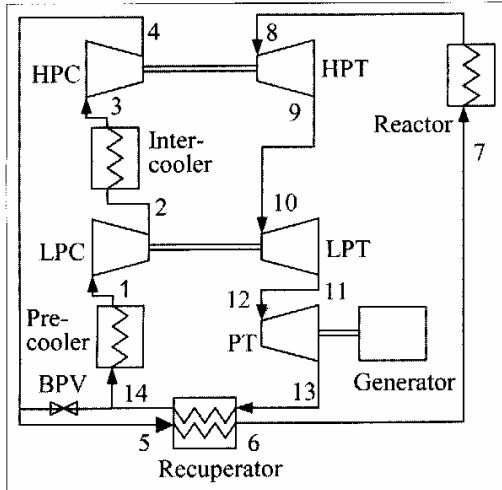


Fig 2. Schematic layout of the PBMR recuperative Brayton cycle.

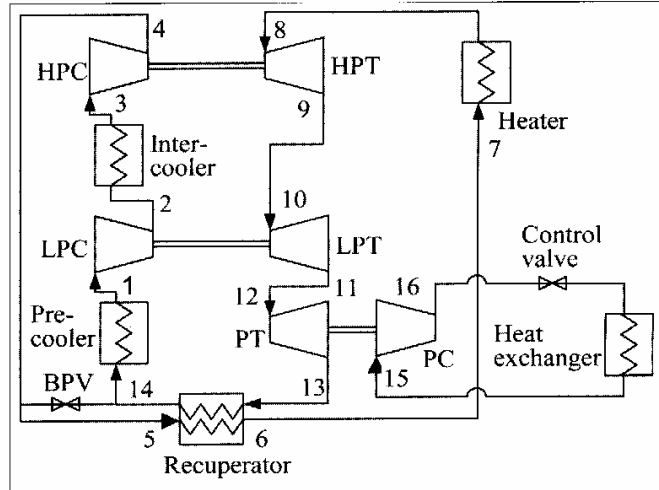


Fig 3. Layout of the micro model cycle.

flow machines. The performance characteristics of centrifugal machines closely resemble that of axial flow machines.

(iii) In the micro model the nuclear reactor is emulated by an electrical resistance heater which, like the pebble bed reactor, has a large thermal capacity.

(iv) The generator is emulated by a load compressor connected to a power dissipation loop consisting of a flow control valve and a heat exchanger as shown in Figure 3. Variations in load are affected by increasing or decreasing the pressure level in the load rejection loop.

First-order cycle analysis

The first step in the design of the micro model was to do a first-order cycle analysis to determine a suitable operating point for the system. Figure 4 and Figure 5 show the result of this analysis with the fol-

lowing assumptions: compressor efficiency = 75 percent, turbine efficiency = 72 percent, pre-cooler and inter-cooler outlet temperature = 26 °C, heater outlet temperature = 700 °C, turbocharger mechanical efficiency = 98 percent, pipe pressure loss = 2 percent of inlet absolute pressure and heat exchanger pressure loss = 10 percent of inlet absolute pressure.

As can be seen from Figure 4, the cycle efficiency increases with recuperator efficiency over the whole range of pressure ratios. At a recuperator efficiency of 1.0 the cycle efficiency decreases with pressure ratio, while it shows an optimum at recuperator efficiencies of smaller than 0.95. Figure 5 shows that the specific work increases with pressure ratio irrespective of the recuperator efficiency.

The recuperator efficiency is a function of the product of the area and the overall heat transfer coefficient of the recuperator and is therefore a design choice. Since the area – and therefore also

the price of the recuperator – increases exponentially with area, an efficiency of approximately 0.85 was chosen as a good compromise between performance and cost. Figure 4 shows that, at a recuperator efficiency of 0.85, the cycle efficiency is a maximum at a pressure ratio of approximately 2.75. Figure 5 on the other hand, shows that the specific work is a maximum at a pressure ratio of approximately 4.5. Since both cycle efficiency and specific work are important and since cycle efficiency is not as sensitive to pressure ratio as specific work, it was decided to design for an overall pressure ratio of approximately 5, which is a good compromise between efficiency and specific work.

Selection of turbochargers

The operating points of the turbo machines are determined by the system operating

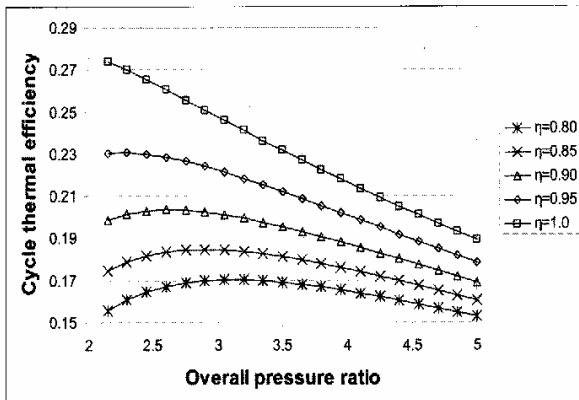


Fig 4. Thermal efficiency as function of recuperator efficiency and overall pressure ratio.

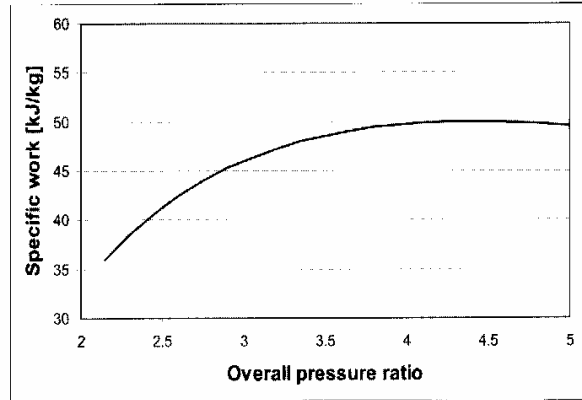


Fig 5. Specific work as function of overall pressure ratio.

Turbo unit	Pressure ratio	Non-dimensional mass flow [kg/s/√K/bar]
Low pressure compressor	2.0	17.3
High pressure compressor	2.0	8.7
High pressure turbine	1.6	8.1
Low pressure turbine	1.7	12.4
Power turbine	1.4	20.0

Tab. 1. Operating points of the different turbo machines for a mass flow of 1 kg/s and LP compressor inlet pressure of 100 kPa.

Turbo unit	Pressure ratio	Non-dimensional mass flow [kg/s/√K/bar]	Power [kW]
Low pressure compressor	2.0	9.3	47.4
High pressure compressor	2.0	4.7	47.4
High pressure turbine	1.6	4.4	48.4
Low pressure turbine	1.7	6.7	48.4
Power turbine	1.4	10.8	27.4

Tab. 2. Pressure ratio, non-dimensional mass flow and power for a mass flow of 0.54 kg/s and LP compressor inlet pressure of 100 kPa.

point and are expressed in terms of pressure ratio and non-dimensional mass flow, which is defined as

$$\dot{m} = \frac{\dot{m} \sqrt{T_0}}{P_0} \quad (1)$$

were \dot{m} = mass flow rate, T_0 = total inlet temperature and P_0 = total inlet pressure. Table 1 shows the pressure ratio and non-dimensional mass flow for a mass flow of 1 kg/s and a system pressure of 100 kPa at the inlet of the low-pressure compressor.

As can be seen from Table 1, the power turbine, although having the lowest pressure ratio, has the largest non-dimensional mass flow. The procedure that was therefore followed was to select the turbocharger with the largest turbine from a range of commercially available units. The turbine of this unit has a non-dimensional mass flow of 10.8 at a pressure ratio of 1.4. This fixes the cycle mass flow at a value of $10.8/20 = 0.54$ kg/s at a pressure level of 100 kPa at the inlet to the LP compressor.

Table 2 shows the recalculated non-dimensional mass flows along with the power rating of the different turbo machines for a cycle mass flow of 0.54 kg/s. The scaling of mass flows does not affect the pressure ratios.

With the pressure ratio and non-dimensional mass flows of the other turbines known from Table 2, turbochargers of which the turbines matched these operating points the closest, were selected. The suitability of the compressors was verified with the aid of Flownet, which

solves for the speed of the different turbochargers.

Modelling of the system with Flownet

Flownet is a general thermal-fluid network analysis code that can model both steady-state and transient flows. Its solver, described elsewhere [1], is based on an Implicit Pressure Correction Method (IPCM) and solves for the conservation of mass and energy at all nodes and momen-

tum in all elements. The code can deal with a wide range of standard network components such as compressors, turbines, pipes, diffusers, valves, heat exchangers and pebble bed nuclear reactors. Flownet can also deal with heat transfer between flow elements and solid structures as well as heat transfer through the solid structures. It should be mentioned that heat exchangers are not handled as lumped systems but as distributed systems [2]. This is necessary to more accurately deal with the thermal capacitance of the metal separating the hot and cold streams. Flownet has been extensively validated against experimental results, other codes and analytical solutions.

Input data of compressors and turbines are provided in the form of performance maps, which gives the pressure ratio, $N/\sqrt{T_0}$, and non-dimensional mass flow, $\dot{m} \sqrt{T_0}/P_0$, for different geometries such as blade angle. Any number of compressor or turbine stages as well as external loads, can be placed on a single shaft. Steady-state load balancing can be affected by varying either the shaft speed or the master turbine geometry, typically the blade angle. In the case of transient flows, Flownet calculates the shaft speed transients by taking the inertia of all rotating parts into account.

Modelling of the cycle by Flownet requires compilation of detail input data for all components such as pipes, diffusers, valves, volumes and heat exchangers. Although space does not allow us to discuss the design of the system in

Heat exchanger	Length between tube sheets [m]	Tube inside diameter [mm]	Number of tubes	Heat transfer area[m ²]	Tube mass [kg]
Pre-cooler	2.1	10.22	575	48	513
Intercooler	1.9	10.22	450	35	363
Load rejection	2.4	10.22	450	43	460
Recuperator	5.8	10.22	1075	255	2728

Tab. 3. Design of the different heat exchangers.

Component	LP compressor inlet pressure = 100 kPa						LP compressor inlet pressure = 250 kPa					
	P _{in} [kPa]	P _{out} [kPa]	T _{in} [°C]	T _{out} [°C]	Rating [kW]	Speed [rpm]	P _{in} [kPa]	P _{out} [kPa]	T _{in} [°C]	T _{out} [°C]	Rating [kW]	Speed [rpm]
LP Compressor	100.0	200.8	22.9	109.6	51.0	72078	250.0	496.9	26.0	112.1	124.3	71811
LP Turbine	248.5	150.5	628.5	549.0	51.0	72078	611.7	372.1	628.8	549.8	124.3	71811
HP Compressor	198.4	381.9	22.9	102.3	46.7	70009	491.3	938.0	26.1	105.1	114.1	69842
HP Turbine	378.0	249.1	700.0	628.5	46.7	70009	929.2	613.2	700.0	628.8	114.1	69842
Power Compressor	105.0	150.7	21.1	65.9	32.1	39073	262.0	372.1	22.9	66.6	76.8	38707
Power Turbine	149.7	105.0	549.0	498.2	32.1	39073	370.2	262.0	549.8	500.4	76.8	38707
Precooler	101.1	100.5	165.3	22.9	83.9	-	252.4	251.2	155.1	26.0	186.6	-
Intercooler	199.1	198.7	109.6	22.9	50.9	-	492.8	491.9	112.1	26.1	124.1	-
Recuperator hot side	103.0	102.3	498.2	165.3	202.6	-	257.1	255.2	500.4	155.1	515.6	-
Recuperator cold side	381.1	379.4	102.3	438.8	202.6	-	935.9	932.5	105.1	453.3	515.6	-
Load rejection HX	106.5	105.1	65.9	21.1	32.1	-	265.1	262.3	66.6	22.9	76.8	-

Tab. 4. Steady-state results for two pressure levels i.e. 100 kPa and 250 kPa at the inlet to the LP compressor.

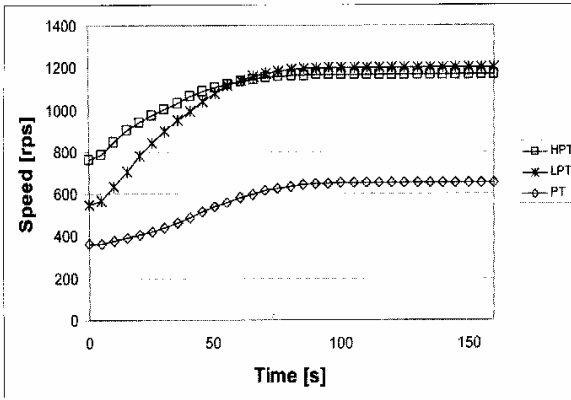


Fig 6. Variation in turbine speed during start-up.

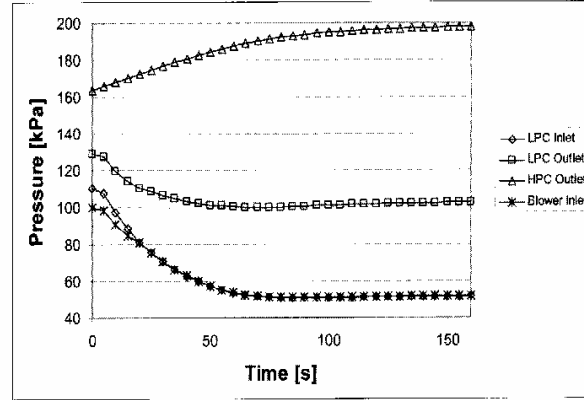


Fig 7. Variation in pressure during start-up.

detail, the diameters of interconnection piping and the design of heat exchangers will be given.

Pipes that connect the major components have a diameter of 200 mm, except the pipe between the power turbine outlet and the recuperator, which has a diameter of 250 mm. All heat exchangers, including the recuperator, are of a shell-and tube design with one shell pass and one tube pass. In the case of the pre-cooler, intercooler and load rejection heat exchanger the gas flows through the tube side with water flowing through the shell side, while in the case of the recuperator the low pressure hot gas coming from the LP turbine flows through the tube side with the high pressure gas from the HP compressor flowing through the shell side.

The details of the different heat exchangers are given in Table 3.

The Flownet steady-state results for two different pressure levels are given in Table 4.

Interesting to note is that the recuperator efficiency is 84 percent in the case of the lower pressure level and 87 percent in the case of the higher pressure level. This is due

to the fact that the flow in the recuperator is laminar at the lower pressure level and turbulent at the higher pressure level.

Simulation of start-up

The system is started by forcing nitrogen through it by an inline blower placed just before the LP compressor while at the same time adding heat in the heater. The simulation starts with the steady-state solution at a point where the heater exit temperature is 400 °C and the LP compressor inlet pressure is 100 kPa. The heat input is now increased at such a rate that the heater exit temperature increases 50 °C/s until the exit temperature reaches a value of 700 °C, whereafter it is kept constant at this value. During this process, the pressure rise across the blower decreases. At the point where the pressure rise becomes zero, the by-pass valve across the blower is opened and the blower is isolated from the main loop. From here onwards the system runs on its own.

Figure 6 shows the variation in turbine speeds and Figure 7 the variation in

pressures during start-up. The speed of all the turbochargers increases as expected and steady-state is reached in approximately 100 s. The pressure at the HP compressor outlet increases, while the pressure at the inlet to the LP compressor decreases. This behaviour is due to the fact that the inventory is kept constant during the start-up.

The time step for this simulation was 0.5 s and execution time was approximately 0.2 s per time step on a 700 MHz Pentium III processor.

Power control

The power output of the system is controlled by increasing or decreasing the mass inventory in the system.

Figure 8 shows the variation in power for the case where the mass is injected and extracted before the LP compressor. The simulation starts at steady-state conditions at a power level of 100 kW (at position 1) and a heater outlet temperature of 700 °C. At time $t = 1$ s mass is injected into the system at a rate of 0.1 kg/s for 400 s where

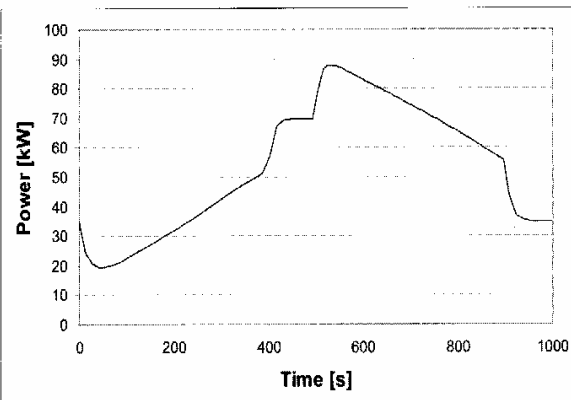


Fig 8. Variation in power when mass is injected and extracted before the LP compressor.

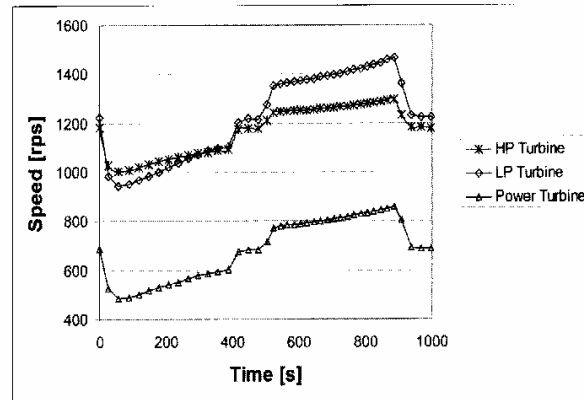


Fig 9. Variation in turbocharger speed when mass is injected and extracted before the LP compressor.

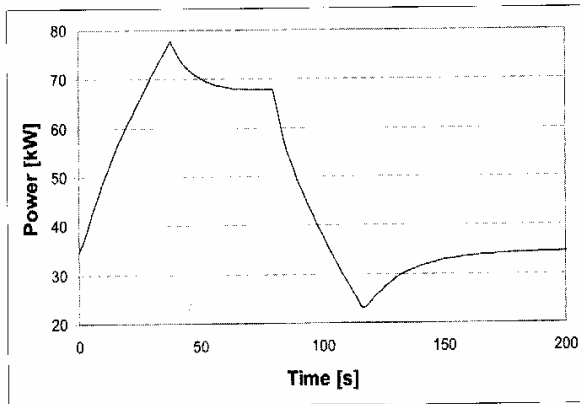


Fig 10. Variation in power when mass is injected and extracted after the HP compressor.

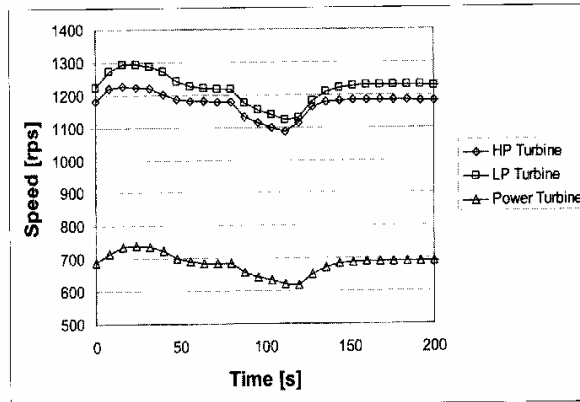


Fig 11. Variation in turbocharger speed when mass is injected and extracted after the HP compressor.

after the system is allowed to stabilise for 100 s. Thereafter mass is extracted at a rate of 0.1 kg/s for another 400 s after which the system is again allowed to stabilise. Figure 8 shows the variation in speed of the three turbochargers during the transient.

Figure 9 shows that the power first decreases before it starts to increase when mass is injected into the system and visa versa. This behaviour, which is undesirable, is due to the immediate increase in the back pressure of the power turbine when one starts to inject mass before the LP compressor. If mass is injected too fast the system can shut-down.

Figure 10 shows the variation in power for the case where the mass is injected and extracted after the HP compressor. The simulation starts at steady-state conditions at a power level of 100 kPa (at position 1) and a heater outlet temperature of 700 °C. At time $t = 1$ s mass is injected into the system at a rate of 1 kg/s for 37 s where after the system is allowed to stabilise for 42 s. Thereafter mass is extracted at a rate of 1 kg/s for another 37 s after which the system is again allowed to

stabilise. Figure 10 shows the variation in speed of the three turbochargers during the transient.

Figure 11 shows that the power output immediately starts to increase when mass is injected after the HP compressor and immediately starts to decrease when mass is extracted. Mass can therefore be injected and extracted at a much faster rate to follow rapid changes in load. Comparing Figures 9 and 11 one can also conclude that the turbocharger speeds do not fluctuate as much in the case of mass injection and extraction at position 4 as compared to injection and extraction at position 1.

Simulations in this section were done for a time step of 0.2 s and execution time was approximately 0.2 s per time step.

Load rejection

Load rejection is done by suddenly opening the bypass valve between the high pressure and low pressure sides, shown in Figure 3. Figure 12 and Figure 13 show the variation in power and speeds of the

turbochargers respectively during a load rejection scenario. The initial condition for this scenario is the steady-state solution for a pressure level of 250 kPa (at position 1 in Figure 3) and a heater outlet temperature of 700 °C.

Figure 10 shows that the power drops from 80 kW to 31 kW (or 61 percent) in approximately 90 s. The valve opening for this case was 15 mm. If the valve opening is increased the system shuts down. Figure 11 shows that the turbocharger speeds also drop significantly during the transient.

Conclusion

The project showed that it is feasible to build a physical model of the PBMR using off the shelf turbochargers. In addition, all the major operating procedures such as start-up, power variation and load rejection were demonstrated on the micro model. The project also demonstrated the utility of a powerful simulation tool such as Flownet in the design of the micro model. □

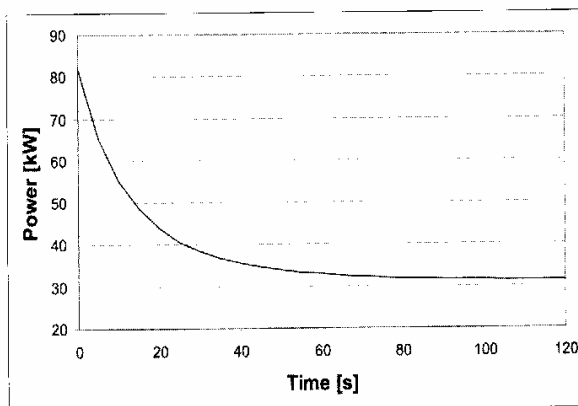


Fig 12. Variation in power during a load rejection.

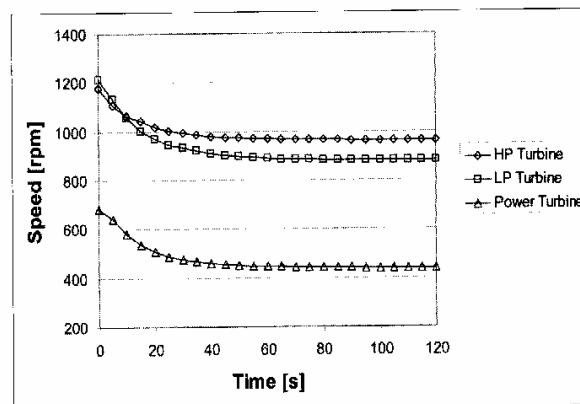


Fig 13. Variation in turbocharger speed during a load rejection.